



ISSN 1823-626X

Malaysian Journal of Fundamental and Applied Sciences

available online at <http://mjfas.ibnusina.utm.my>



Numerical Simulation on Convection-Diffusion in an Overlapping Stenosed Artery

Ilyani Abdullah*, Amira Husni Talib and Siti Noor Izzati Che Mohd Sabri

Department of Mathematics, Faculty of Science & Technology, UMT, 21030 Kuala Terengganu, Terengganu, Malaysia

Received 15 December 2012, Revised 30 March 2013, Accepted 28 April 2013, Available online 6 May 2013

ABSTRACT

Consider an unsteady Newtonian blood flow coupled with mass transport in which flowing through an artery with the presence of an overlapping stenosis. The flowing blood is governed by nonlinear partial differential equations while the convection-diffusion equation to blood is employed to couple with the Newtonian equation in order to characterize the mass transport of blood-borne components such as low-density lipoprotein (LDL). This mass transport refers to the movement of blood-borne molecules from flowing blood into the artery wall, or vice versa. These coupled equations are solved numerically using finite-difference method with an appropriate prescribed initial and boundary conditions. The graphical results of velocity profiles and mass concentration of the solute are presented along the distributions over the entire considered arterial segment. These results show the important role of mass transport in stenosed artery.

| Newtonian fluid flow | Mass transport | Overlapping stenosis | Finite difference method |

© 2013 Ibnu Sina Institute. All rights reserved.
<http://dx.doi.org/10.11113/mjfas.v9n3.102>

1. INTRODUCTION

Mass transport of blood-borne is referred to the movement of macromolecules, such as low-density lipoprotein (LDL) and oxygen, between the flowing blood and the arterial wall. It is claimed by [1] that the transport of these macromolecules has been linked to atherogenesis, the formation of subintimal plaques in the lining of arteries. As noted by [2], the occurrence of mass transfer between blood flow and arterial wall is caused by the pressure difference across the luminal surface. At certain sites in arterial system, the localization of atherosclerosis lesions is developed in human. Furthermore, the study by [3] showed that blood rheology could significantly affect the most parts of aorta with high luminal surface of LDL concentration. The mass transport on stenosed and non-stenotic artery has been investigated in [1], [4]-[7] and some researchers considered a fluid-wall multilayer model ([8]-[10]).

The deposition of LDL is said to be one of the cause of atherosclerosis, a process of progressive thickening and hardening of the arterial wall due to the accumulation plaque (stenosis) on the inner linings of arteries. Over the time, the arteries become constricted, their elasticity disappears and it reduces the blood volume that travels through the arteries. This will lead to lack of oxygen and nutrients transportation to the peripheral organs. Most of the studies in mass transport so far have been focused in the presence of single stenosis ([1], [5]-[7]). In order to have a one step closer to the real situation, an overlapping stenosis is suggested to be considered subject to pulsatile pressure

gradient. As reported by [11], the problem becomes more acute in the presence of an overlapping stenosis instead of single stenosis. The study has been extended by [12] considering the time-dependent geometry of an overlapping stenosis in tapered artery. While [13] gave special attention to multistenoses which appear in the artery.

The goal of this study is to investigate the distribution of the velocity and mass concentration in an overlapping stenosed artery. The governing equations, together with the prescribed conditions, are solved using finite-difference scheme.

2. MATHEMATICAL FORMULATION

2.1 Governing Equations

Let us consider (r, z, θ) be the coordinates of a material point in the cylindrical coordinates system where the z -axis is taken along the arterial segment while r and θ are taken along the radial and the circumferential directions, respectively. The geometry is assumed to be axisymmetric ($\partial/\partial\theta=0$) and the azimuthal velocity component vanishes. In the absence of external forces, the dimensionless continuity and momentum equations which govern the blood flow in the cylindrical coordinates system may be written as:

*Corresponding author. E-mail: ilyani@umt.edu.my

$$\frac{\partial u}{\partial r} + \frac{u}{r} + \frac{\partial w}{\partial z} = 0 \tag{1}$$

$$\frac{\partial u}{\partial t} + u \frac{\partial u}{\partial r} + w \frac{\partial u}{\partial z} = -\frac{\partial p}{\partial r} + \frac{1}{\text{Re}} \left(\frac{\partial^2 u}{\partial r^2} + \frac{1}{r} \frac{\partial u}{\partial r} - \frac{u}{r^2} + \frac{\partial^2 u}{\partial z^2} \right) \tag{2}$$

$$\frac{\partial w}{\partial t} + u \frac{\partial w}{\partial r} + w \frac{\partial w}{\partial z} = -\frac{\partial p}{\partial z} + \frac{1}{\text{Re}} \left(\frac{\partial^2 w}{\partial r^2} + \frac{1}{r} \frac{\partial w}{\partial r} + \frac{\partial^2 w}{\partial z^2} \right) \tag{3}$$

where u and w are the dimensionless radial and axial velocity components, respectively, t is the dimensionless time, p is the dimensionless pressure, Re is the Reynolds number which is defined by $\text{Re} = r_0 U_0 \rho / \mu$, with r_0 is the normal radius in the arterial segment, U_0 is the cross-sectional average velocity, ρ is the density of blood, and μ is the viscosity. The lumen radius, R , is assumed to be sufficiently smaller than the vessel segment, L , which stated as $R \ll L$, then it is simply reduced to $\partial p / \partial r = 0$, which means that the pressure p in cross section is independent of radial coordinate. This assumption has been made by ([14] - [16]) and it is well supported by [17]. In eq. (3), the pressure gradient in the axial direction, $\partial p / \partial z$ has been taken for human beings which is given by

$$-\frac{\partial p}{\partial z} = A_1 + A_2 \cos \omega t, \quad \text{for } t > 0 \tag{4}$$

with A_1 is the constant amplitude of the pressure gradient, A_2 is the amplitude of the pulsatile component giving rise to systolic and diastolic pressure, and $\omega = 2\pi f$, f is the pulse frequency.

The dimensionless mass transport is governed by the convection-diffusion equation and is written as

$$\frac{\partial C}{\partial t} + u \frac{\partial C}{\partial r} + w \frac{\partial C}{\partial z} = \frac{1}{\text{Re} \cdot \text{Sc}} \left(\frac{\partial^2 C}{\partial r^2} + \frac{1}{r} \frac{\partial C}{\partial r} + \frac{\partial^2 C}{\partial z^2} \right) \tag{5}$$

where C is the concentration, and Sc is the Schmidt number which is defined by $\text{Sc} = \mu / (\rho D)$, D is the coefficient of diffusion

2.2 Initial and Boundary Conditions

These are the assumptions that have been used to prescribe the boundary of the problem:

- a. Initially no flow takes place when the system is at rest ($t=0$),
 $w(r, z, 0) = u(r, z, 0) = C(r, z, 0) = 0$.

- b. Along the axis of symmetry ($r=0$), the axial velocity gradient, the normal component of the velocity and the mass concentration gradient vanish,

$$\frac{\partial w(r, z, t)}{\partial r} = u(r, z, t) = \frac{\partial C(r, z, t)}{\partial r} = 0.$$

- c. At the arterial wall ($r=R$), the axial velocity and the mass concentration vanish, while the radial velocity is prescribed by no-slip condition,
 $w(r, z, t) = C(r, z, t) = 0, \quad u(r, z, t) = \frac{\partial R}{\partial t}$.

- d. The flow is assumed to be fully developed with parabolic profile of velocity at the inlet ($z=0$), and the mass concentration is assumed to be constant,

$$w(r, z, t) = \left(1 - \frac{r^2}{R^2} \right) \left[1 + g \sin \left(\frac{\alpha^2}{\text{Re}} t \right) \right]$$

$$u(r, z, t) = 0, \quad C(r, z, t) = 1.$$

g is the dimensionless amplitude while α is the Womersley number, $\alpha = r_0(\omega \rho / \mu)^{1/2}$.

- e. At the outlet ($z=L$), L is the finite length of arterial segment, the velocity gradients and mass concentration gradient are taken to be traction-free conditions,

$$\frac{\partial w(r, z, t)}{\partial z} = \frac{\partial u(r, z, t)}{\partial z} = \frac{\partial C(r, z, t)}{\partial z} = 0.$$

2.3 Geometry of Stenosis

The geometry of an overlapping stenosed artery is given by

$$R(z, t) = \begin{cases} \left[1 - \frac{\tau_m}{l_0}(z-d) \left\{ 11 - \frac{94}{3l_0}(z-d) + \frac{32}{l_0^2}(z-d)^2 - \frac{32}{3l_0^3}(z-d)^3 \right\} \right] \frac{a(t)}{R_0}, & d \leq z \leq d + \frac{3}{2}l_0 \\ \frac{a(t)}{R_0}, & \text{otherwise} \end{cases} \tag{6}$$

with $R(z, t)$ denotes the dimensionless radius of the arterial segment in the constricted region. Meanwhile, R_0 is the constant radius of the normal artery in the non-stenotic region, l_0 is 2/3 of the length of the stenosis, d is the location of the stenosis onset and τ_m is taken to be the critical height of the stenosis. Figure 1 shows the schematic diagram of an overlapping stenosed artery.

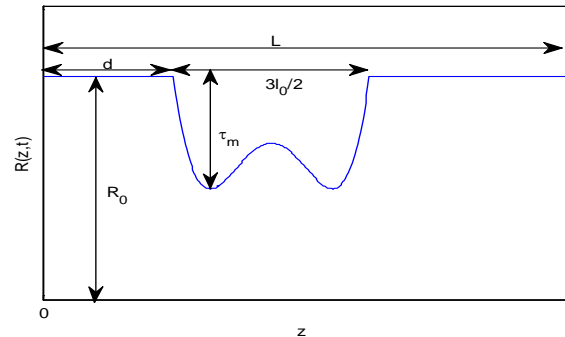


Fig. 1 Geometry of a stenosed artery with $R_0=0.152$, $\tau_m=0.2R_0$, $l_0=1$, $d=0.5$.

The time-variant parameter in (6) is given by

$$a(t) = 1 - h(\cos \omega t - 1)e^{-hot}$$

where h is a constant and $\omega = 2\pi f$. This time-dependent parameter is introduced to suit the flexible stenosis and it is relevant to the unsteady flow mechanism under stenotic conditions. The flexibility is known to be related in some manner to the amount of collagen, elastin and smooth muscle present at a particular point.

2.4 Numerical Procedure

In order to avoid difficulty of prescribed moving surface of boundary conditions, let us introduce the radial coordinate transformation,

$$x = \frac{r}{R(z,t)}$$

The value of x is from 0 to 1. This transformation has the effect of immobilizing the vessel wall in the transformed coordinate x and allows the difficulties stemming from some kinematic boundary conditions prescribed for a moving surface to be overcome. The transformed form of continuity, momentum and convection-diffusion equations are:

$$\frac{1}{R} \frac{\partial u}{\partial x} + \frac{u}{xR} + \frac{\partial w}{\partial z} - \frac{x}{R} \frac{\partial R}{\partial z} \frac{\partial w}{\partial x} = 0 \tag{7}$$

$$\begin{aligned} \frac{\partial u}{\partial t} - \frac{x}{R} \frac{\partial R}{\partial t} \frac{\partial u}{\partial x} + \frac{u}{R} \frac{\partial u}{\partial x} + w \left(\frac{\partial u}{\partial z} - \frac{x}{R} \frac{\partial R}{\partial z} \frac{\partial u}{\partial x} \right) \\ = -\frac{\partial p}{\partial r} + \frac{1}{\text{Re}} \left[\frac{1}{R^2} \frac{\partial^2 u}{\partial x^2} + \frac{1}{xR^2} \frac{\partial u}{\partial x} - \frac{u}{(xR)^2} \right] \end{aligned} \tag{8}$$

$$\begin{aligned} \frac{\partial w}{\partial t} - \frac{x}{R} \frac{\partial R}{\partial t} \frac{\partial w}{\partial x} + \frac{u}{R} \frac{\partial w}{\partial x} + w \left(\frac{\partial w}{\partial z} - \frac{x}{R} \frac{\partial R}{\partial z} \frac{\partial w}{\partial x} \right) \\ = -\frac{\partial p}{\partial z} + \frac{1}{\text{Re}} \left[\frac{1}{R^2} \frac{\partial^2 w}{\partial x^2} + \frac{1}{xR^2} \frac{\partial w}{\partial x} + \left(\frac{r}{R} \frac{\partial R}{\partial z} \right)^2 \frac{\partial^2 w}{\partial x^2} \right. \end{aligned} \tag{9}$$

$$\left. + \left[\frac{2x}{R^2} \left(\frac{\partial R}{\partial z} \right)^2 - \frac{x}{R} \frac{\partial^2 R}{\partial z^2} \right] \frac{\partial w}{\partial x} + \frac{\partial^2 w}{\partial z^2} \right]$$

$$\begin{aligned} \frac{\partial C}{\partial t} - \frac{x}{R} \frac{\partial R}{\partial t} \frac{\partial C}{\partial x} + \frac{u}{R} \frac{\partial C}{\partial x} + w \left(\frac{\partial C}{\partial z} - \frac{x}{R} \frac{\partial R}{\partial z} \frac{\partial C}{\partial x} \right) \\ = \frac{1}{\text{Re-Sc}} \left[\frac{1}{R^2} \frac{\partial^2 C}{\partial x^2} + \frac{1}{xR^2} \frac{\partial C}{\partial x} + \left(\frac{r}{R} \frac{\partial R}{\partial z} \right)^2 \frac{\partial^2 C}{\partial x^2} \right. \end{aligned} \tag{10}$$

$$\left. + \left[\frac{2x}{R^2} \left(\frac{\partial R}{\partial z} \right)^2 - \frac{x}{R} \frac{\partial^2 R}{\partial z^2} \right] \frac{\partial C}{\partial x} + \frac{\partial^2 C}{\partial z^2} \right]$$

With the transformation, the initial and boundary conditions are transformed as follows:

at $t=0$: $w(x, z, 0) = u(x, z, 0) = C(x, z, 0) = 0$

at $x=0$: $\frac{\partial w(x, z, t)}{\partial x} = u(x, z, t) = \frac{\partial C(x, z, t)}{\partial x} = 0$

at $x=R$: $w(x, z, t) = u(x, z, t) = C(x, z, t) = 0$

at $z=0$: $w(x, z, t) = (1-x^2) \left[1 + g \sin \left(\frac{\alpha^2 t}{\text{Re}} \right) \right]$

$u(x, z, t) = 0, C(x, z, t) = 1$

at $z=L$: $\frac{\partial w(x, z, t)}{\partial z} = \frac{\partial u(x, z, t)}{\partial z} = \frac{\partial C(x, z, t)}{\partial z} = 0$

The radial velocity is obtained by solving Eq. (7) instead of Eq. (8), for the sake of simplicity. Some workout can be referred in [18]. Thus we have

$$u(x, z, t) = x \left[\frac{\partial R}{\partial z} w + \frac{\partial R}{\partial t} (2-x^2) \right] \tag{11}$$

The finite difference scheme for solving Eq. (9-11) is based on the central difference approximations for all the uniform spatial derivatives and the forward difference formula for time derivative. Thus we obtained the discretized form:

$$u_{i,j}^{k+1} = x_j \left[\left(\frac{\partial R}{\partial z} \right)_i^k w_{i,j}^{k+1} + \left(\frac{\partial R}{\partial t} \right)_i^k (2-x_j^2) \right] \tag{12}$$

$$\begin{aligned} w_{i,j}^{k+1} = w_{i,j}^k + \Delta t \left[-\left(\frac{\partial p}{\partial z} \right)^{k+1} + \left\{ \frac{x_j}{R_i^k} \left(\frac{\partial R}{\partial t} \right)_i^k + \frac{x_j}{R_i^k} \left(\frac{\partial R}{\partial z} \right)_i^k w_{i,j}^k - \frac{u_{i,j}^k}{R_i^k} \right\} \left(\frac{\partial w}{\partial x} \right)_{i,j}^k \right. \\ \left. - w_{i,j}^k \left(\frac{\partial w}{\partial z} \right)_{i,j}^k + \frac{1}{\text{Re}^2 (R_i^k)^2} \left\{ \left[1 + \left(x_j \left(\frac{\partial R}{\partial z} \right)_i^k \right)^2 \right] \left(\frac{\partial^2 w}{\partial x^2} \right)_{i,j}^k \right. \right. \right. \\ \left. \left. + \left[\frac{1}{x_j} 2x_j \left(\left(\frac{\partial R}{\partial z} \right)_i^k \right)^2 - x_j R_i^k \left(\frac{\partial^2 R}{\partial z^2} \right)_i^k \right] \left(\frac{\partial w}{\partial x} \right)_{i,j}^k + (R_i^k)^2 \left(\frac{\partial^2 w}{\partial z^2} \right)_{i,j}^k \right\} \right] \end{aligned} \tag{13}$$

$$\begin{aligned} C_{i,j}^{k+1} = C_{i,j}^k + \Delta t \left[\left\{ \frac{x_j}{R_i^k} \left(\frac{\partial R}{\partial t} \right)_i^k + \frac{x_j}{R_i^k} \left(\frac{\partial R}{\partial z} \right)_i^k w_{i,j}^k - \frac{u_{i,j}^k}{R_i^k} \right\} \left(\frac{\partial C}{\partial x} \right)_{i,j}^k \right. \\ \left. - w_{i,j}^k \left(\frac{\partial C}{\partial z} \right)_{i,j}^k + \frac{1}{\text{Re}^2 (R_i^k)^2} \left\{ \left[1 + \left(x_j \left(\frac{\partial R}{\partial z} \right)_i^k \right)^2 \right] \left(\frac{\partial^2 C}{\partial x^2} \right)_{i,j}^k \right. \right. \right. \\ \left. \left. + \left[\frac{1}{x_j} 2x_j \left(\left(\frac{\partial R}{\partial z} \right)_i^k \right)^2 - x_j R_i^k \left(\frac{\partial^2 R}{\partial z^2} \right)_i^k \right] \left(\frac{\partial C}{\partial x} \right)_{i,j}^k + (R_i^k)^2 \left(\frac{\partial^2 C}{\partial z^2} \right)_{i,j}^k \right\} \right] \end{aligned} \tag{14}$$

We have $u(x_j, z_i, t_k)$, $w(x_j, z_i, t_k)$ and $C(x_j, z_i, t_k)$ which are defined by

$x_j = (j-1)\Delta x, \quad j = 1, 2, \dots, N+1$ such that $x_{(N+1)} = 1$

$z_i = (i-1)\Delta z, \quad i = 1, 2, \dots, M+1$

$t_k = (k-1)\Delta t, \quad k = 1, 2, \dots$

3. RESULTS & DISCUSSION

The results are obtained using the following parameters values (which taken from ([1], [6], [7], [11], [18])): $R_0=0.152, l_0=1, d=0.5, L=4, \tau_m=0.1R_0$ (refers to a mild

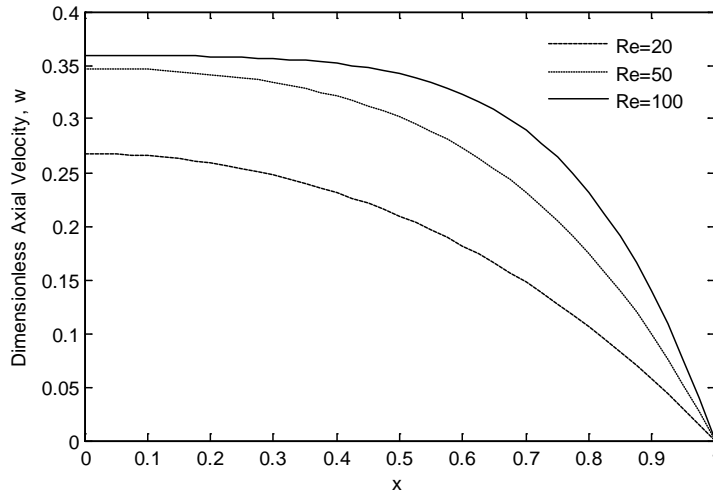


Fig. 2 The dimensionless axial velocity for different Re.

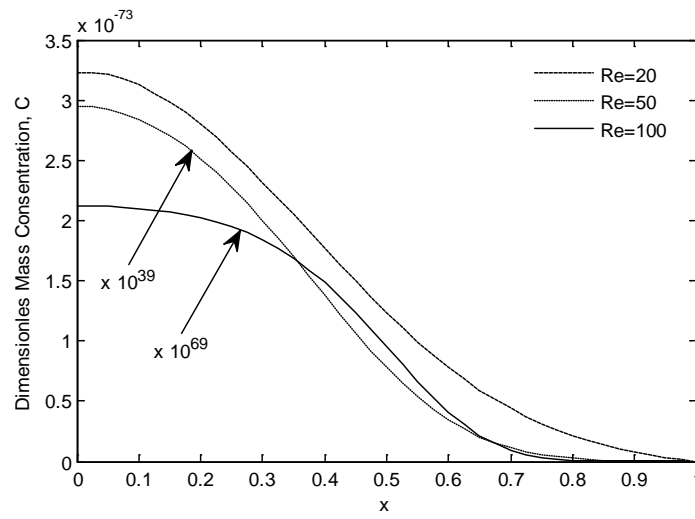


Fig. 3 The dimensionless mass concentration for different Re.

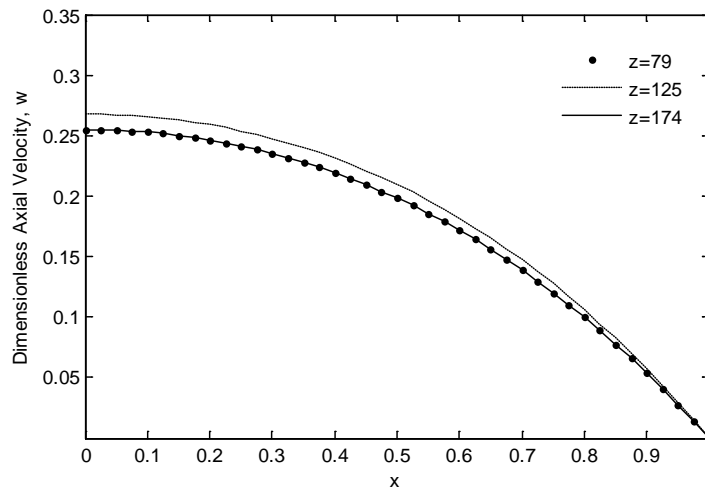


Fig. 4 The dimensionless axial velocity at different location.

stenosis), $g=0.1$, $h=0.1$, $f=1.2$, $A_1=3$, $A_2=0.2A_1$, $Sc=3$; using these values, we obtained the numerical results for velocity and mass concentration. For computational domain, solutions are computed by the grid size 400×40 for z and x , respectively. Fig. 2 depicts the results for dimensionless axial velocity with different Re , where Re is defined by the ratio of the inertial forces to viscous forces. It quantifies the relative importance of these two types of forces for a given flow conditions. Higher value of Re defines as when the inertial forces dominates, it reduces the effect of viscous force thus becoming insignificant. The chosen values of Re are based on studies by [1]; [6] and [7]. From Fig. 2, when $Re=100$, the profile of velocity is more flat in shape. It shows that the convective term dominates where the term is driven by the inertial forces. When Re becomes smaller, the value of blood velocity reduces, as we assumed that the density and viscosity of blood are constant for Newtonian fluid.

Fig. 3 shows the distribution of dimensionless mass concentration along the radial axis with different Re . The mass concentration is gradually decrease from the axis towards the wall, which we have zero mass concentration on the arterial wall. This is due to the assumption that the diameter of LDLs is larger than the endothelial cellular gaps, thus the LDL diffusion to the arterial wall is negligible and convective-diffusive LDL mass balance between lumen and arterial wall. However, as stated in some studies in humans, pigeons and rabbits ([19]-[21]), the flux of LDL from plasma into the arterial wall depends on the plasma concentration of LDL and LDL permeability at the plasma-arterial wall interface. And [22] noted that even for a low plasma LDL concentration may experience a relatively high flux of LDL into the arterial wall if the LDL permeability of the arterial wall is high, which is not considered in the present study. This emphasizes that further understanding of permeability of the arterial wall is needed.

As in Fig. 4, the profiles of dimensionless axial velocity are shown at three distinct locations for $Re=20$. The chosen z which are $z=79$ and $z=174$ refer to the first and second critical heights of the overlapping stenosis, while $z=125$ is in the middle between the two critical points, with smaller height of stenosis (refer Fig.1). Both critical heights give the same value of velocity and velocity is greater at smaller height of stenosis. It is clearly shows that the presence of stenosis could significantly reduces the blood velocity.

4. CONCLUSION

A mathematical model of pulsatile blood flow, considering the mass transfer, through an overlapping stenosis has been studied. The convection-diffusion equation is coupled with Newtonian model represents the

mass concentration in the vessel. Thus, we have another view of flow-field besides the velocity profile itself. It gives us understanding how the mass concentration is distributed along the radial axis. Furthermore, the presence of considered overlapping stenosis, which mimics the real situation, reduces the amount of velocity. It has been shown that the stenosis really affects the flowing blood.

ACKNOWLEDGEMENT

The authors thank the Universiti Malaysia Terengganu for funding the project (vot TPM 68006/2011/14).

REFERENCES

- [1] A. Valencia and M. Villanueva, *Int. Comm. Heat and Mass Transfer*, 33 (2006) 966-975.
- [2] S. Fazli, E. Shirani and M.R. Sadeghi, *J. of Biomechanics*, 44 (2011) 68-76.
- [3] L. Xiao, F. Yubo, D. Xiaoyan and Z. Fan, *J. of Biomechanics*, 44 (2011) 1123-1131.
- [4] C.G. Caro, J.M. Fitz-Gerald and R.C. Schroter, *Proc. Of Royal Soc. London, Ser. B Biological Science*, 177 (1970) 109-159.
- [5] L.H. Back, J.R. Radbill and D.W. Crawford, *J. of Biomechanics*, 10 (1977) 763-774.
- [6] M.R. Kaazempur-Mofrad, S. Wada, J.G. Myers and C.R. Ethier, *Int. J. of Heat and Mass Transfer*, 48 (2005) 4510-4517.
- [7] Sarifuddin, S. Chakravarty, P.K. Mandal and H.I. Andersson, *Z. angew. Math. Phys.*, 60 (2009) 299-323.
- [8] N. Sun, N.B. Wood, A.D. Hughes, S.A.M Thom and X.Y. Xu, *Am. J. of Physiology Heart and Circulatory Physiology*, 292 (2007) H31148-H33157.
- [9] N. Yang and K. Vafai, *Int. J. of Heat and Mass Transfer*, 51 (2008) 497-505.
- [10] S. Chung and K. Vafai, *J. of Biomechanics*, 45 (2012) 371-381.
- [11] S. Chakravarty and P.K. Mandal, *Math. Comp. Modelling*, 24 (1996) 43-58.
- [12] S. Chakravarty and P.K. Mandal, *Int. J. Non-linear Mechanics*, 35 (2000) 779-793.
- [13] S. Chakravarty and A.K. Sannigrahi, *Math. Comp. Modelling*, 29 (1999) 9-25.
- [14] S.C. Ling and H.B. Atabek, *J. of Fluid Mechanics*, 55 (1972) 493-511.
- [15] E. Belardinelli and S. Cavalcanti, *J. of Biomechanics*, 25(11) (1992) 1337-1349.
- [16] S. Cavalcanti, *J. of Biomechanics*, 28 (1995) 387-399.
- [17] M.D. Deshpande, D.P. Giddens and R.F. Mabon, *J. of Biomechanics*, 9 (1976) 165-174.
- [18] I. Abdullah and N. Amin, *Math. Meth. Appl. Sci.*, 33 (2010) 1910-1923.
- [19] C.E Niehaus, A. Nicoll, R. Wootton, B. Williams, J. Lewis, D.J. Coltart and B. Lewis, *Lancet*, 2 (1977) 469-471.
- [20] B.G. Nordestgaard, H.A. Tybjaerg and B. Lewis, *Arterios. Thrombosis*, 12 (1992) 6-18.
- [21] D.C. Schwenke and R.W. St. Clair, *Arterios. Thrombosis*, 13 (1993) 1368-1381.
- [22] L.B. Nielsen, *Atherosclerosis*, 123 (1996) 1-15.